Scholars Bulletin *(Engineering)*

An Official Publication of "Scholars Middle East Publishers" ISSN 2412-9771 (Print)
Dubai, United Arab Emirates ISSN 2412-897X (Online)
Website: www.saudijournals.com

Recent Vapour-Liquid Condensation Phenomena Challenges in Annular Tube

W. M. Faizal W. A. Rahim[1,2], C.Y. Khor[1], M.Z. Zainon[2,3], N.N.N. Ghazali[2]

[1]Department of Mechanical Engineering Technology, Faculty of Engineering Technology, University Malaysia Perlis, 02100 Padang Besar, Perlis, Malaysia

[2]Department of Mechanical Engineering, Faculty of Engineering, University of Malaya, 50603 Kuala Lumpur, Malaysia

[3]Center of Energy Science, University of Malaya, 50603 Kuala Lumpur, Malaysia

***Corresponding author**
M.Z. Zainon

Article History
Received: 03.04.2018
Accepted: 12.04.2018
Published: 30.04.2018

DOI:
10.36348/sb.2018.v04i04.003

Abstract: This paper presents a review of the recent challenges on vapour-liquid condensation phenomena inside the annular tube. The condensation phenomenon is a main concern in nuclear power plant safety system. The condensation in annular tube is a complex phenomenon, which can classify into two categories: (i) condensation in liquid (Direct Contact Condensation) and (ii) condensation on the plate. In Newton's Law Cooling, heat transfer surface area and surface temperature (i.e., bubble or plate) are the main parameters that need to be concerned. The heat surface area of condensation in annular tube can be determined by investigating void fraction for the desire flow pattern. In this article, the condensation phenomena are reviewed based on the amount of substantial research work conducted from the past decades to the present. Condensation phenomena in annular tube such as type of phase change, interfacial heat transfer, influence of flow structure and void fraction measurement method, are considered in the review. The future need and challenges of vapour-liquid condensation in an annular tube are also highlighted in this article.

Keywords: Condensation, direct contact condensation, flow pattern, void fraction, annular tube.

INTRODUCTION

Two-phase flow and phase change phenomena in a tube are usually observed in the power plant, heat exchanger, and condenser in industrial application.

The system's design is crucial to ensure the safe operation, especially in nuclear power plant. Therefore, a good understanding of two-phase flow and phase change phenomena is important when to improve and redesign the system. Nowadays, the world demanding high accuracy of the phase change phenomena monitoring technique to enhance the performance of the nuclear power plant.

Multifarious scholars had carried out the new experiments to make enhancements for the current available method in understanding the behaviour of condensation phenomena. Besides, the simulation modelling technique also has been employed to model and visualize the two-phase flow phenomenon. Through this simulation technique, the mechanism of phase change and condensation can be visualized in a real time. These efforts motivate the current literature review that focus on the condensation behaviour in a tube. This article is expected to provide profound understanding on the effect of the flow behaviour or pattern to the condensation and determination of condensation phenomena in the experiment.

In the beginning of the article, the condensation in a tube is focused based on the previous articles, which have been reported by previous scholars. Besides, this article also provide an overview of condensation in two-phase flow in a tube. Mostly, the researchers considered water-vapour to reveal the behaviour of condensation in a tube flow. This article also includes the review of substantial experimental work related to the determination of the condensation in a tube. Two streams of determination of condensation were pursued and reviewed: one towards the experiment currently used in determining the condensation in a tube and the other towards the potential new experiment that could be used to determine the condensation in a tube. Furthermore, some of the unique challenges and future needs in determining the vapour-liquid condensation through the void fraction technique are also discussed in this paper.

Overview of Condensation Phenomena

Condensation involves phase change phenomena, which is a complex field in the heat transfer area. Two-phase changes (i.e., gases or vapour and liquid or water) were studied in various applications, such as microchannel, rocket

vehicle, heat exchanger and air conditioning system. The medium for phases reflected in the application are summarized in **Table-1**. In the early stages of research, the condensation phenomena were introduced by Nusselt [1] and he proposed the first theoretical solution to solve the heat transfer coefficient by assuming the linear temperature profile across the laminar film thickness of the liquid. To understand the condensation phenomena, convection Newton's Law of cooling needs to be referred (Eq. 1), as the fundamental theory in analysing the phenomena.

$$Q = hA_v(T_v - T_w) \quad (1)$$

Where

Q[W] is heat, h $[Wm^{-2}K^{-1}]$ is heat transfer coefficient, A_v $[m]$ is vapour area, $T_v[k]$ is vapour temperature and $T_w[k]$ is water temperature.

Table-1: Summary Type of Phases Involve in Condensation

Researcher	Phases	Application	Experimental	Flow Pattern
Chengbin Z *et al.*, [2]	ethanol–water	Modern Devices (Microchannel)	High Speed Camera	Droplet-slug/bubble Pure slug/bubble Annular-streak Annular flow
Xu Q *et al*., [3]	Steam-water	Liquid-propellant rocket vehicle	High Speed Camera	Steam jet condensation
Gou J *et al*., [4]	Steam-water	Passive safety system (Heat exchanger)	Analytical	Film condensation
Azizi S and Ahmadloo E [5]	Gas-liquid (R134a)	Air conditioning system	Analytical (Artificial Neutral Network)	Film condensation

By considering the water temperature much more lower than vapour; the vapour area will decrease as followed by the occurrence of the condensation phenomenon. This phenomenon is a condensation occurs along the tube because of the mass vapour phase been transferred to the water phase. For phase change phenomenon, the heat transfer rate is equal to the rate of heat transfer from vapour to water [6], as shown in equation (2), where, $h_{fg}[J\ kg^{-1}K^{-1}]$ is latent heat of vaporization and $\dot{m}_c[kg\ s^{-1}]$ is the mass of condensation rate.

$$h(T_v - T_w)A_v = \dot{m}_c h_{fg} \quad (2)$$

Rearranging the equation (2), condensation heat transfer coefficient, $h[Wm^{-2}K^{-1}]$ from vapour to water can be obtained as shown below,

$$h = \dot{m}_c h_{fg}/A_v(T_v - T_w) \quad (3)$$

As the vapour enter the tube in the superheated vapour condition, the modified latent heat of vaporization (for subcooling condition) is integrated with the superheated effect and is given in equation (4), where, T_{sat} is a saturation temperature at the interface of vapour. The second term refers to the subcooling of the water and the last term is referred to the cooling from superheated vapour to the saturated temperature.

$$h_{fg}^{*} = h_{fg} - 0.68c_{pl}(T_{sat} - T_w) + c_{pg}(T_v - T_{sat}) \quad (4)$$

Referring to the equation (3), the area (A_v) is referred to the vapour area which occurring from two-phase flow structure either bubbly flow, slug flow, churn flow or annular flow. All type of flows will have various shapes that are very complicated to measure the surface areas contains the injected vapour energy. In the single phase flow, convection force practically used dimensionless parameter such as Nusselt number (Eq. 5), Reynolds Number (Eq. 6), Prandtl number (Eq. 7) and Jacob number (Eq. 8) as defined as:

$$Nu = \frac{h\bar{d}_v}{k_w} \quad (5)$$

$$Re = \frac{\rho_w v_v \bar{d}_v}{\mu_w} \quad (6)$$

$$P_r = \frac{v_w}{a_w} \quad (7)$$

$$Ja = \frac{\rho_w c_{pw} \Delta T}{\rho_v (h_v - h_w)} \quad (8)$$

Where
h_v and h_w are the specific enthalpy of steam and water. To estimate the vapour equivalent diameter, d_v, the formula is shown in this equation (9). But for two-phase flow, the time variation of the vapour external surface that directly contact with subcooling liquid can be defined as by assuming that vapour shape is single bubble is derived by Yao W *et al.*, [7]:

$$\frac{dA_v}{dt} = 2\pi d_v \frac{d(d_v)}{dt} \quad (9)$$

The equations (2), (3), (5), and (6) indicate that the importance of the area and diameter of vapour in tube flow in the determination of condensation heat transfer coefficient and mass transfer rate. The understanding of flow pattern in tube either bubble flow, bubbly-slug flow, slug flow, and annular flow (**Figure-1**) is vital to analyse the phenomena in two-phase flow to determine the area and diameter of vapour.

For two-phase flow, a vapour area in flow pattern will consider as void fraction. Determination of void fraction is a main focus for the researcher and currently demanding high accurate determination technique in two-phase flow and phase change phenomena. The main parameters in two-phase flow, such as correlation of void fraction, flow pattern maps, and slip velocity are also discussed in this article. Before further explores the phenomenon in the two-phase flow and phase change, the understanding of the interfacial heat transfer formulation is important to analyse the heat transfer of two-phase flow and condensation in a tube. Thus, section 3 summarizes the continuity equation, momentum equation and energy equation that have been used to analyse the two-phase flow in the previous studies.

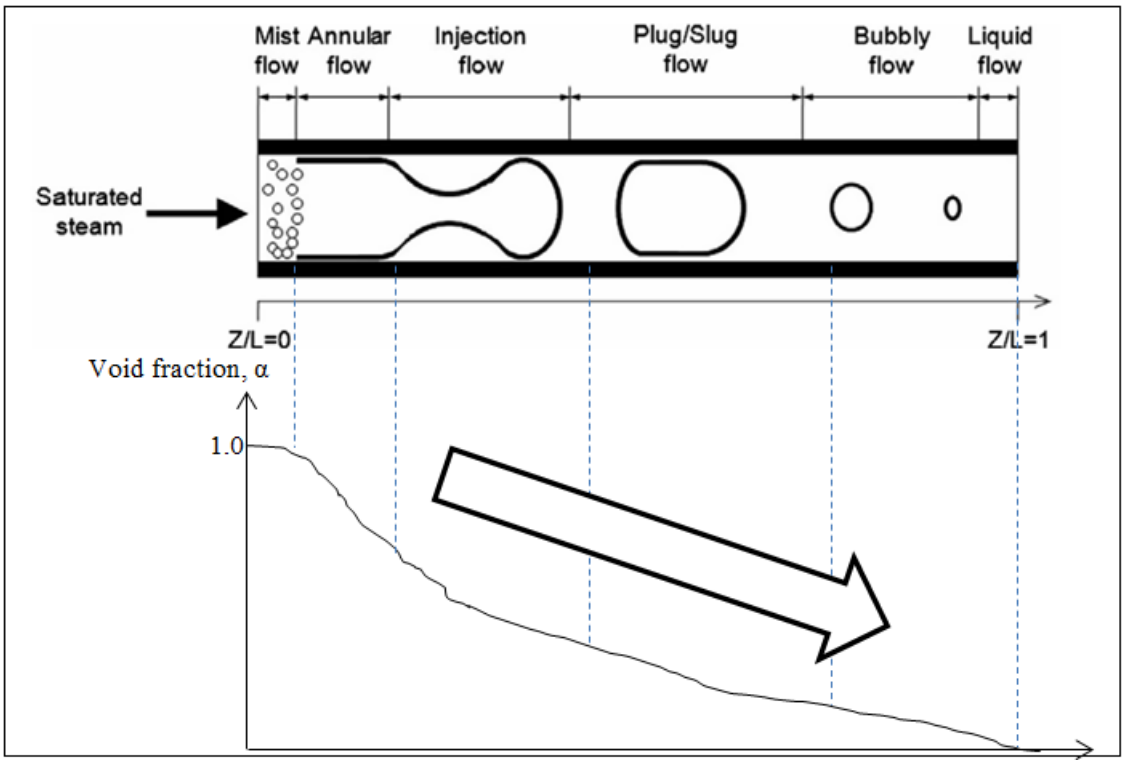

Fig-1: Condensation flow pattern inside tube [8]

Interfacial Heat Transfer formulation

Heat transfer in tube flow had been studied in early 1949 by Tangreen *et al.*, [9]. In the early stage of investigation, a lot of assumption was used to simplify the research and solve using analytical techniques. Albagli and Gany [10] derived the two-phase continuity equation (Eq. 10). Nowadays the analysis of two-phase flow heat transfer can be done either analytical [11, 12], experimentation [13, 14] or simulation [15-17]. The understanding of the fundamental equation is crucial for researcher to reveal the correlation between the variables in the heat transfer phenomena, especially in the analysis of two-phase heat transfer of tube flow. The continuity equation, momentum equation and the energy equation in two-phase flow [10] provide better understanding in the fundamental internal force convection in tube flow. Moreover, the heat transfer can be analysed through the correlation approach in empirical and

semi-empirical that can be divided into three situations, which are two-phase multiplier based models [18], interfacial shear stress based models [19] and boundary layer based models [4].

Continuity Equation

The continuity equation in the two-phase flow can be expressed by equation (10):

$$\dot{m}_{tot} = (1 + \mu_o)\rho_l u_{lo} A_o = [\alpha\rho_v u_v + (1 - \alpha)\rho_l u_l]A \quad (10)$$

Where

μ_o is a local mass flow ratio between the vapour and water $[kg\ s^{-1}]$, ρ_l, is a density of the liquid $[kgm^{-3}]$, u_v and u_l, are the velocity for vapour and liquid phase $[ms^{-1}]$, A is cross sectional area of the tube $[m^2]$, α is void fraction, and subscript 'o' is referred to the initial condition for the flow in a tube. μ is a local ratio mass flow rate between vapour phase and liquid phase as shown in equation (11).

$$\mu = \frac{\dot{m}_v}{\dot{m}_l} \quad (11)$$

Void fraction is the ratio between gas areas in the liquid flow over total area of the flowing fluid. This parameter is the most important part to analyse the condensation in the annular channel. In one dimensional flow, fundamental assumptions need to be made to simplify the analysis. Therefore, average parameters are assumed over the cross-section and this average model is termed as the drift flux model. Thus the void fraction can be expressed in the basic equation.

$$\alpha = \frac{1}{1+\frac{\rho_v u_v}{\mu\rho_l u_l}} = \frac{A_v}{A} \quad (12)$$

Hence,

$$\frac{d\alpha}{dx} = -\frac{1}{1+\frac{\rho_v u_v}{\mu\rho_l u_l}}\left(-\frac{\rho u}{\mu}\frac{d\mu}{dx} + u\frac{d\rho}{dx} + \rho\frac{du}{dx} - \frac{\rho u}{u_l}\frac{du_l}{dx}\right) \quad (13)$$

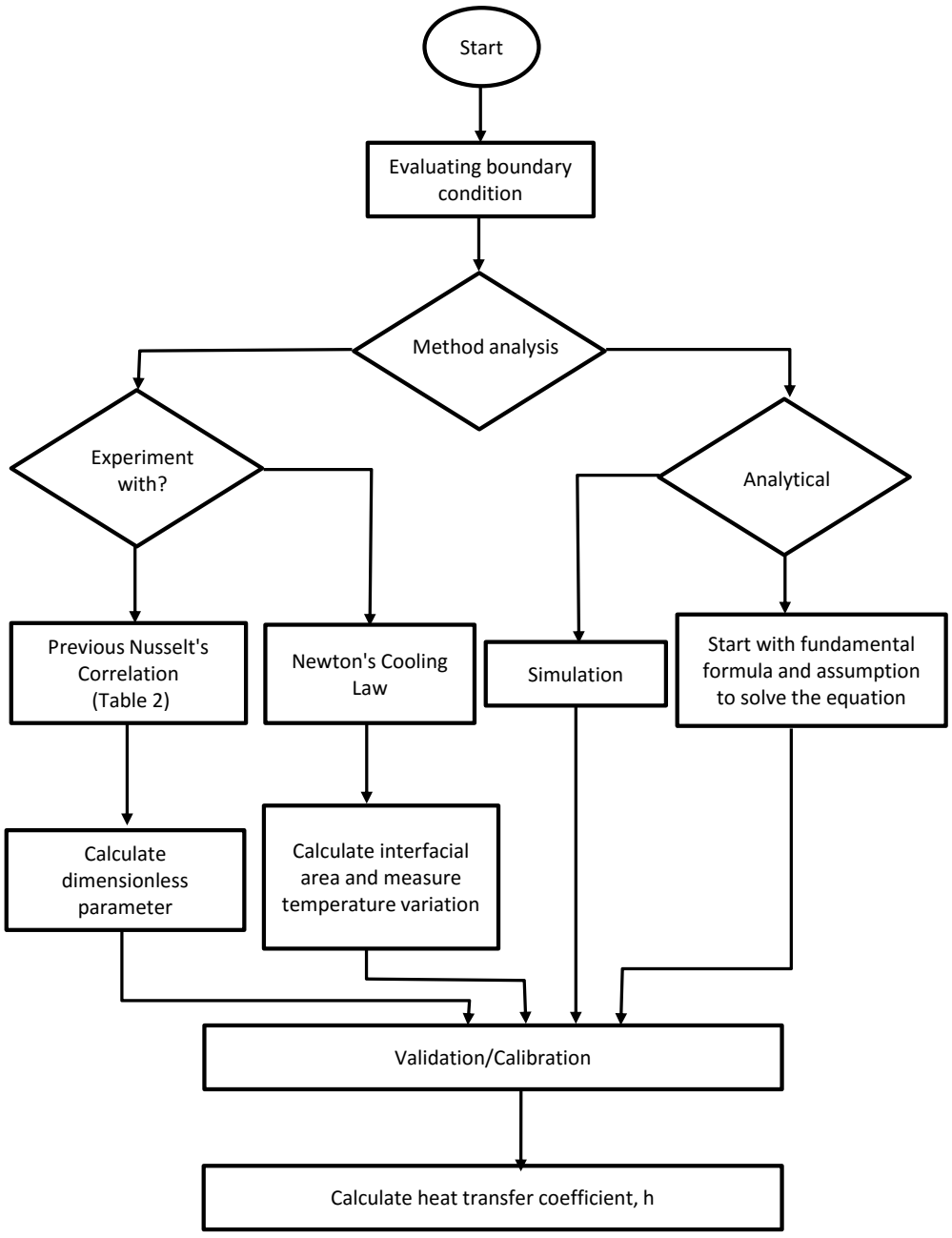

Fig-2: Flowchart to analyse the condensation phenomena inside the tube

Momentum Equation

Momentum equation is used to describe the friction force's effect exerted on the fluid by tube wall. This equation shows the effect of shear stress in the last term of equation (14) denoted by τ. In equation (15), the frictional coefficient and two-phase flow correlation factor are represented by f and Φ^2.

$$\alpha\rho u\frac{du}{dx}+(1-\alpha)\rho_l u_l\frac{du_l}{dx}=\ -\frac{d}{dx}[\alpha P+(1-\alpha)P_l]-\frac{4\tau}{d} \qquad (14)$$

Rearranging Equation (14):

$$\frac{dp_l}{dx}=-\frac{1}{1-\alpha}\left[\alpha\frac{dP}{dx}+\alpha\rho u\frac{du}{dx}+(1-\alpha)\rho_l u_l\frac{du_l}{dx}+(P-P_l)\frac{d\alpha}{dx}\right]-\frac{2\rho_l u_l^2}{d}f\Phi^2 \qquad (15)$$

In two-phase flow heat transfer, the momentum change is attributed by the material transport from vapour phase to the surroundings, which due to the condensation (Eq.16) phenomenon.

$$\rho u\frac{du}{dx}+\frac{1}{2}\rho_l\left(u\frac{du}{dx}-u_l\frac{du_l}{dx}\right)=-\frac{dP_l}{dx}-\frac{\frac{1}{2}C_D\rho_l\pi r^2|u-u_l|(u-u_l)}{\frac{4}{3}\pi r^3}-\delta\frac{u(u-u_l)}{\frac{4}{3}\pi r^3}\frac{1}{\dot{n}}\frac{d\dot{m}}{dx} \qquad (16)$$

Vapour bubble will affect by the drag factor as shown in equation (16), because of the interaction of vapour phase surface to the surrounding and it can be calculated by the following correlation for the condensation:

$$C_D=\frac{24}{Re}\left(1+\frac{3}{16}Re\right);\ Re\le 1 \qquad (17a)$$

$$C_D=10^{(1.455-0.912log_{10}Re)};\ 1<Re\le 4 \qquad (17b)$$

$$C_D=\frac{18.5}{Re^{0.6}};\ 4<Re\le 500 \qquad (17c)$$

$$C_D=0.444\ ;\ Re\ >500 \qquad (17d)$$

Thermal Energy Equation

Energy equation (Eq.18) describes the heat transfer between the bubble phase (i.e., bubble, bubbly-slug, slug, annular flow) to the liquid phase in the tube, where, h is condensation heat transfer coefficient $[Wm^{-2}K^{-1}]$, and c_p is vapour phase specific heat $[Jkg^{-1}K^{-1}]$.

$$4\pi r^2h(T_l-T)=(1-|\delta|)\frac{4}{3}\pi r^3\rho c_p u\frac{dT}{dx}+\delta h_{fg}u\frac{1}{\dot{n}}\frac{d\dot{m}}{dx} \qquad (18)$$

In order to describe the changes of vapour phase radius, the ideal gas equation (19) is considered and substitutes into the equation (18) and rearrange to become equation (20).

$$P=\rho RT \qquad (19)$$

$$\frac{dr}{dx}=\frac{h(T_l-T)}{\rho u h_{fg}}+\frac{r}{3R}\frac{dR}{dx}-\frac{r}{3P}\frac{dP}{dx}+\frac{r}{3T}\frac{dT}{dx} \qquad (20)$$

When the condensation takes place in the tube flow between vapour and liquid phase, equation (20) is mainly used to analyse the changing of the vapour radius that describes the condensation phenomena.

The determination of condensation or phase change phenomena has been reviewed based on the most related substantial works. The vapour radius in the condensation or phase change phenomena can be calculated through the analytical method (Eq.20). This equation taking account many assumptions [10] to observe the phase change phenomena. However, the result of the equation is inadequate to reflect the real situation. To increase the reliability and accuracy of the result, experimental method [20-23] is the best approach to understanding the condensation behaviour in tube flow and also can be used to verify the fundamental equation. In two-phase flow, the trend of void fraction will reduce and alter during the condensation along the tube. Understanding the heat transfers of each flow structure and relationship with void fraction along the annular tube is significant in the research area of two-phase flow heat transfer.

In reality, the visualization of a real two-phase mixtures flow inside the pipe is very difficult. In relation to this problem, numerous researchers had put in their efforts to overcome this shortcoming. They have proposed various techniques, which will be discussed in the following section for different purposes such as void fraction measurement, flow pattern identification, velocity measurement, etc. From the substantial studies on relationship and correlation for the two-phase flow, the flowchart to analyse the condensation phenomena inside tube is constructed as illustrated in Figure 2. As a result, it can be employed to determine the flow characteristic of the system through various methods (i.e., analytical, experimental and simulation).

Heat Transfer in Different Flow Structures

The flow patterns or flow regimes give a crucial impact on some flow characteristics, such as heat transfer conditions, velocity profile and pressure fluctuation. The classification of the flow regime is useful for researcher but sometimes it becomes subjective to be defined. Several flow regimes have been identified and defined by researchers. Various appropriate names have been given with the suitable definition based on the acceptable behaviour of the patterns and shapes of the bubble. The definitions for each type of flow pattern were given according to the flow direction of the

two-phase flow. Besides, Hewitt and Robertson [24] defined the co-current vertical upward flow of vapour-liquid in a vertical pipe for various regimes.

Flow pattern Mapping

The vertical upward two-phase flow, particularly those involving boiling phenomena, has a significant engineering application. To illustrate the flow pattern in such condition, it is best to refer to flow boiling in a vertical annulus as reported by Collier [25]. As shown in **Figure 1** (in Section 2), the illustration of tube depicts the entire structure of flow boiling from the incipient boiling until dry out.

The bubbly flow begins at the early stage during the onset of boiling bubble nucleation particularly with the effect of sub-cooling. At this point, bubbles were generated (nucleated) within the superheated thermal boundary layer on the wall of the heated surface but later on getting condensed in the core of the flow. Sometime, the onset of nucleation might happen in a poor or delayed manner due to low vapour qualities and low heat flux in sub-cooled boiling. Slug waves were formed after the bubbly flow. As the flow boiling reaches the upper part of the heated surface, the liquid has received enough energy to change phase in a more frequent rate. As a result, the annular flow regime is formed with the thin liquid film flow on the wall, vapour in the core, and droplet entrainment with the alternate deposition flow along with the vapour core.

All transitions of flow regime as discussed above can be explained or estimated for prediction studies using the flow pattern map. It is a complete diagram that shows interchange of boundaries between patterns. There were a lot of arguments involving the two-phase studies on the selection of fair and appropriate parameters to be presented in the flow pattern maps, particularly on scaling the transition boundaries. Generally, it can be displayed by using dimensionless parameters representing the superficial velocity of liquid and gas, in the form of normal scale or log-log axis. One of the famous examples of flow pattern as reported by Hewitt and Robertson [24]. This map represents the result of small flow channel but there is also a non-dimensional pairs of parameter as in Fair [26] and, Dalkilic and Wongwises [27] studies. The map is applicable for all conditions of channel diameter and other diameters also can be applied in the experimental study. Moreover, another popular mapping of flow pattern was proposed by Taitel and Duklear [28].

Interfacial Heat Transfer in two phase flow

Phase change phenomena in the heat transfer or interfacial heat transfer occur during the boiling, evaporation and condensation. Interfacial heat transfer inside the tube is depending on the interaction of gas phases. In flow pattern maps, the transition curve can be read as the transition of patterns or transition zone that gives the analogy of transition between laminar and turbulent flow as well. As shown by previous scholars, the parameters used by scholars differ from one to another. To utilize the Fair's [26] map, we should have the superficial velocities of gas and liquid on x-axis and mass flow rate on y-axis. These superficial velocities and mass flow rate are then to be matched vertically and horizontally to reach the intersection of the graph. The same procedure is applied in order to utilize Hewitt *et al*., [24] map but we should have different parameters. In the two-phase flow studies, many more flow pattern maps were developed with various information that can be obtained from those maps, such as comprehensive treatment provided by Barnea *et al*., [29] and fluid viscosity by Furukawa and Fukano [30]. Kattan *et al*., [31] and Zurcher *et al*., [32] presented the flow map for a diverse range of parameters such as, vapour qualities, mass velocities and heat fluxes. This map also provided the information on the estimation of dry out point at the upper side of the tube for evaporation and extended for other fluids, refrigerant HFC-134a, HFC407c and R717 (ammonia).

Flow mapping suggested by Taitel and Duckler [28] and, Furukawa and Fukano [30] typically used as a reference since these two maps are in the range of experiment works for vapour phase (steam) and liquid (water) flow structure and orientation. Furthermore, the tube position, the geometry of the tube, vapour and liquid flow rate and the physical properties of the phases also give a role in determination of flow pattern and it will give the significant finding on the condensation phenomena inside the tube [33].

In the vertical orientation, the researchers investigated the condensation in many ways, such as direct contact condensation, which means the vapour and liquid interact without having a wall. Besides, the condensation occurs on the surface during the low temperature liquid flow that separate from the vapour was alienated by the wall. In heat transfer of two phase flow, the flow structure, such as bubbly flow, slug flow, churn flow and annular flow inside the tube occur in direct contact condensation. Dalkilic *et al*., [33] claim that the heat transfer between phases is depending on the interaction and flow structure. This indicates that the studies of heat transfer on the flow structure provide an overall understanding of condensation inside the tube. Rouhani and Axelsson [34] found the condensation coefficient, h_c linearly correlates with both interfacial area and local liquid Reynolds number. Hence, they proposed the correlation to calculate the condensation rate (equation 21):

$$h_c = aA_b Re_l \qquad (21)$$

where a is a proportional constant and may depend on thermal and physical properties of liquid and vapour phases with the value of $10^{-11} kg/m^3 sK$. A_b is a liquid-vapour interfacial area per unit length of the tube, and Re_l correspond to the liquid Reynolds number obtained from the local liquid velocity as,

$$Re_l = \frac{GD_e}{(1-\alpha)\mu_l} \qquad (22)$$

Referring to the equation 21 (h_c), interfacial area varies sensitively according to the flow pattern. Liang and Peter Grifith [35] used transient conduction-diffusion model to analyse condensation inside tube and assume that the bubble volume to be characterized by the injector size, which can be expressed by $V_v = cD_i^3$. Kalman and Mori [36] also investigated the significance of drag coefficient that involve in bubble condensing in subcooled liquid and they are assuming the vapour bubble in the spherical shape [37-43]. Equation (22) was used to estimate the heat transfer coefficient in the tube for a single bubble. In this equation, the rate of bubble collapse $d\hat{R}/dt$ can be calculated from the derivation of polynomial fitted to the data of each collapse process. Meanwhile, Kim and Park[44] derived the condensation heat transfer with this term dV_b/dt to show the bubble condensation rate is expressed in equation (23), respectively. Thus, equation (24) can be used to estimate the bubble collapse along the tube for a single vapour.

$$h = -\rho_v h_{fg} \frac{R_o}{\Delta T} \frac{d\hat{R}}{dt} \qquad (23)$$

$$h = \frac{\rho_v h_{fg} (dV_b/dt)}{A_b \Delta T_{sub}} \qquad (24)$$

Table-2 summarizes the formulations of the Nusselt number to measure the effectiveness of heat transfer, which have been used in various applications that mainly dependent on the Reynolds and Prandtl number of the flow inside the annular tube. These correlations mainly depend on the flow pattern. Aforementioned in the previous section, void fraction is the main properties in the two phase flow but the study on this scope is still limited in the literature. The correlation between the void fraction and the heat transfer coefficient still remain a huge research gap. Moreover, the annular flow pattern heat transfer will use Log Mean Temperature Different (LMTD) in calculating the heat transfer coefficient [45].

Table-2: Correlation of flow pattern and condensation heat transfer

Authors	Equation	Bubble History

Bubbly/Slug flow		
Iseberg and Sideman [46]	$Nu = \frac{h_c D_b}{k_l} = 1/\sqrt{\pi} Re_v^{1/2} Pr^{1/3}$	$\beta = \left(1 - 3/\sqrt{\pi} JaRe_{BO}^{1/2} Pr^{1/3} Fo_0\right)^{2/3}$
Akiyama [47]	$Nu = \frac{h_c D_b}{k_l} = 0.37 Re_v^{0.6} Pr^{1/3}$	$\beta = \left(1 - 2.8 \times 0.37 Re_{bo}^{\frac{1}{2}} Pr^{\frac{1}{3}} JaFo_o\right)^{\frac{1}{1.4}}$
Chen and Mayinger [48]	Before detachment $Nu = \frac{h_c D_b}{k_l} = 0.61 Re_v^{0.6} Pr^{1/2} \beta^{0.3}$ After detachment $Nu = \frac{h_c D_b}{k_l} = 0.851 Re_v^{0.7} Pr^{1/2} \beta^{0.3}$	$\beta = \left(1 - 0.56 Re_{bo}^{1/3} JaFo_o\right)^{0.9}$
Zeitoun *et al*., [49]	$Nu = \frac{h_c D_b}{k_l} = 2.04 Re_v^{0.61} \alpha^{0.328} Ja^{0.308}$	$\beta = (1 - 5.67 Re_{bo}^{0.61} \alpha^{0.328} Ja^{0.698} Fo_o) Pr^{0.72}$
Ranz and Marshall [50]	$Nu = \frac{h_c D_b}{k_l} = 2 + 0.6 Re_v^{0.5} Pr_l^{0.3}$	$0 \leqq Re \leqq 200$
Hughmark [51]	$Nu = \frac{h_c D_b}{k_l} = 2 + 0.6 Re_v^{0.5} Pr_l^{0.33}$ $Nu = \frac{h_c D_b}{k_l} = 2 + 0.6 Re_v^{0.5} Pr_l^{0.33}$	$1 \leqq Re \leqq 450$ $0 \leqq Pr_l < 250$ $1 \leqq Re < 1000$ $0 \leqq Pr_l \leqq 250$
Kim and Mudawar [52]	$Nu = \frac{h_c D_b}{k_l} = \left[\left(0.048 Re_f^{0.69} Pr_f^{0.34} \frac{\phi_g}{X_{TT}}\right)^2 + \left(3.2 \times 10^{-7} Re_f^{-0.38} Su_{go}^{1.39}\right)^2\right]^2$ $X_{TT} = \left(\frac{\mu_f}{\mu_g}\right)^{0.1} \left(\frac{1-x}{x}\right)^{0.9} \left(\frac{\rho_g}{\rho_f}\right)^{0.5}$ $\phi_g^2 = \frac{(dP/dz)_f}{(dP/dz)_g}$	
Warrier *et al*., [53]	$Nu = \frac{h_c D_b}{k_l} = 0.6 Re_v^{\frac{1}{2}} Pr_l^{\frac{1}{3}} (1 - 1.20 Ja^{9/10} Fo^{2/3}$	$20 < Re_v < 700$ $1.8 < Pr_l < 2.9$ $12 < Ja < 100$ $\beta = 1 - 1.8 Re_{bo}^{\frac{1}{2}} Pr_l^{\frac{1}{3}} JaFo_0 (1 - 0.72 Ja^{0.9} Fo^{\frac{2}{3}})$

Table 2: Correlation of condensation heat transfer and flow pattern

Authors	Equation	Remark

Annular Flow	
Akers *et al*., [54]	$Nu = \frac{h_c D_b}{k_l} = 0.026 Pr_l^{1/3} \left\{ G \left[(1-x) + x \left(\frac{\rho_l}{\rho_v} \right)^{0.5} \right] \frac{D_h}{\mu_f} \right\}^{0.8}$
Cavallini and Zecchin [55]	$Nu = \frac{h_c D_b}{k_l} = 0.05 Re_f^{0.8} Pr_f^{0.33} \left[1 + \left(\frac{\rho_f}{\rho_g} \right)^{0.5} \left(\frac{x}{1-x} \right) \right]^{0.8}$
Shah [56]	$Nu = \frac{h_c D_b}{k_t} = 0.023 Re_f^{0.8} Pr_f^{0.4} \left[(1-x)^{0.8} + \frac{3.8 x^{0.76} (1-x)^{0.04}}{P_R^{0.38}} \right]$
Haraguchi *et al*., [57]	$Nu = \frac{h_c D_b}{k_l} = 0.0152 \left(1 + 0.6 Pr_f^{0.8}\right) \frac{\phi_g}{X_{TT}} Re_f^{0.77} X_{TT}$ $= \left(\frac{\mu_f}{\mu_v} \right)^{0.1} \left(\frac{1-x}{x} \right)^{0.9} \left(\frac{v_f}{v_g} \right)^{0.5} \phi_g$ $= 1 + 0.5 \left[\frac{G}{\sqrt{g \rho_g (\rho_f - \rho_g) D_h}} \right]^{0.75} X_{TT}^{0.35}$
Dobson and Chato [58]	$Nu = \frac{h_c D_b}{k_l} = 0.023 Re_f^{0.8} Pr_f^{0.4} \left(1 + \frac{2.22}{X_{TT}^{0.89}} \right)$
Wang *et al*., [59]	$Nu = \frac{h_c D_b}{k_l} = 0.027 Pr_f Re_f^{0.6792} x^{0.2208} \frac{\phi_g}{X_{TT}} \phi_g^2 = 1.376 + 8 X_{TT}^{1.665}$
Koyama *et al*., [60]	$Nu = \frac{h_c D_b}{k_l} = 0.0152 \left(1 + 0.6 Pr_f^{0.8}\right) \frac{\phi_g}{X_{TT}} Re_f^{0.77} \phi_g^2$ $= 1 + 21[1 - \exp(-0.319 D_h)] X_{TT} + X_{TT}^2$

Interfacial Area in Two Phase Flow

Interfacial area is a crucial variable in determining the interfacial heat transfer for all flow patterns. Determination of the interfacial area inside the flow channel is the important part but it is impossible due to several limitations. Referring to the Figure-2 (in Section 2), interfacial area is also considered as a main variable in determination heat transfer coefficient for condensation phenomena in the inside tube flow. Thus, it is important to make clear the correlation and assumption when calculating the interfacial area. Figure-3 shows the approach that reported by Lin and Hibiki [61] that categorizes the bubble in two-phase flow into two groups. Ma *et al*., [62] studied the interfacial area that affected in bubbly flow for vertical orientation and Yang et al. [63] focused on the interfacial area for the thermal hydraulic rod bundle. Conjunction the importance of observing the condensation inside the tube, interfacial area is the main variable that needs to be further investigated. However, interfacial area cannot directly determine from the experiment and it needs to consider the correlation that introduced by Rohatgi and Saha [64]. They also highlight the importance of void fraction in the determination of interfacial area. Conversely, void fraction can directly determine from the experiment by using several methods that are reviewed in following section. Rohatgi and Saha [64] proposed the correlation of the interfacial area per unit volume accordingly to various flow patterns:

Bubbly flow

$[\alpha < 0.3 \text{ or } \alpha < 0.5 \text{ with } G > 2700 kg/m^2 s]$

$$A_b = \frac{6 \alpha \rho_l V_{gl^2}}{We\ \sigma} \qquad (25)$$

Slug flow

$[0.3 < \alpha < 0.5 \text{ with } G < 2500 kg/m^2 s]$

$$A_b = \frac{3(0.92-\alpha) \rho_l V_{gl^2}}{We\ \sigma} + \frac{5(3\alpha - 0.9)}{D_e} \qquad (26)$$

where *We* is Weber Number (dimensionless number), σ is a surface tension of liquid (N/m), D_e is the hydraulic diameter (m) and V_{gl} is weighted mean vapour drift velocity (m/s), which for upwards steam-water bubbly-churn flow:

$$V_{gl} = 1.41 \left[\frac{\sigma g (\rho_l - \rho_v}{\rho_{l^2}} \right]^{0.25} \qquad (27)$$

and α is the corresponding void fraction obtained by Zuber and Findlay [65], as in equation 28.

$$\alpha = x/\left[C_o\left(x\frac{\rho_l-\rho_v}{\rho_l}+\frac{\rho_v}{\rho_l}\right)+\frac{\rho_g V_{gl}}{G}\right] \qquad (28)$$

Where C_o is the vapour distribution (C_o = 1.13) and G is mass velocity, (kg/m^{2}s). Toda and Hori [66] examined the condensation using video imaging process and they found the difficulties to estimate the interfacial area inside the tube flow along the test section. The interfacial area of void fraction is useful in analysing the flow phenomena of the nuclear reactor safety system [61-63]. The interfacial correlation is summarized in Table-3.

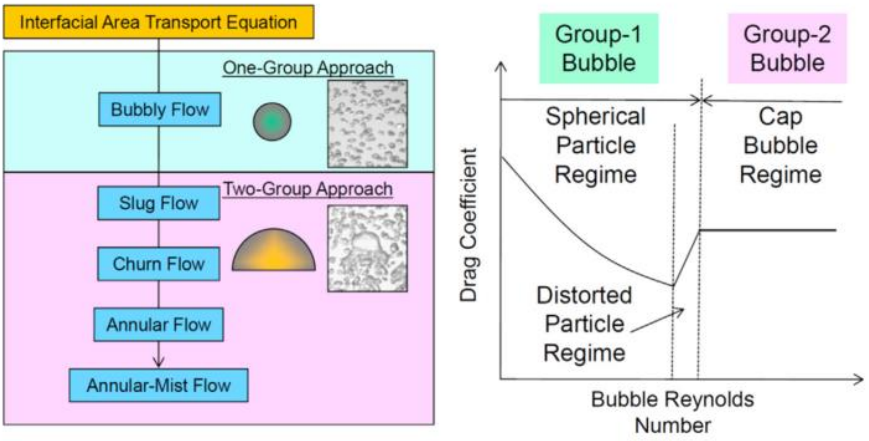

Fig-3: Illustration of two bubble groups analysis for two-phase flow [61]

Table-3: Interfacial correlation

Authors	a_i, interfacial correlation
Kasturi and Stepanek [67]	$\frac{a_i \dot{V}_l}{1-\alpha} = 2.26\times10^{-5}(dP/dz)_f^{1.07}$
Akita and Yoshida [68]	$a_i = \left(\frac{gD_h^2\rho_l}{\sigma}\right)^{1/2}\left(\frac{gD_h^3}{v_f^2}\right)^{0.1}\frac{\alpha^{1.13}}{3D_h}$
Tomida *et al*., [69]	$a_i = 0.22\left(\frac{dP}{dz}\right)_l \alpha$ for $j_v < 8ms^{-1}$

Determination of void fraction via experiment

Void fraction is a main variable in the two-phase flow phenomena. The importance of void fraction had been discussed by many researchers in the determination and observation of condensation inside a tube [70-73]. Furthermore, industrial applications that involve the two-phase flow and heat transfer as discussed earlier, usually having flow transfer in many arrangements of piping system. In real application, most of them (i.e., two phase flow) are not visible, since they are not in a transparent tube. The complexity of two-phase flow patterns, however, needed to be identified to gain detailed information on a particular application. Therefore, the detection, monitoring and full description of flow patterns are required since it contributes to the many influences on the flow parameters. This can be carried out via experimental work with proper monitoring elements and must be documented in a proper manner. For example, the measurement of various parameter distributions in space and time (e.g., velocity, density and pressure) as studied by Keska and William [74]. Therefore, referring to the equation (24), this indicates the importance of the determination of the vapour area to calculate the condensation and heat transfer coefficient in annular channel. By using the interfacial area correlation that proposed by researchers [75, 76], the interfacial area could be determined easily by knowing the void fraction inside the annular channel. To overcome this issue, void fraction and interfacial area can be considered as the best approach to solve the heat transfer coefficient in two-phase flow. Nowadays, various modern measurement techniques such as electrical [77-79], gamma ray [80, 81] and ultrasound [82, 83] have been employed to measure the void fraction of vapour-liquid flow inside the annular channel. Thus, the following sub-sections are the reviews on the current and potential experimental methods to determine the void fraction in the two-phase flow for the vapour-water condition.

Visual Observation

A few techniques have been developed and applied to identify the flow patterns. Visual observation is a very easy and common method to visualize the flow pattern through the captured image or video. Generally, the flow pattern is often acquired by photographic image of the flow, which can be directly captured or recorded from the experiment. This technique had been used by Taylor *et al*., [84] to study the flow pattern inside a transparent tube. Many researchers

used this technique since it is a straight forward method and with recent technologies that enable the moving flow to be recorded and examined carefully after the experiment. It will be easier for co-current flow but a little challenging for counter current flow. Kim et al. [85] presented some results on the flow pattern by using this method to the measure the rising of a slug.

A high-speed photography technique is crucial to visualize the high velocity flows. Other unique techniques were used when the experiment involves high pressure and high temperature flows. However, the major drawback of visual observation method is light refraction. When the light transmits through the transparent tube, the flow was subjected to a complex series of refraction, thus the images produced are often confusing. This situation making it difficult to construe the flow information. Therefore, the visualization system requires a high technology camera that has a high shuttle speed feature. For video visualization, a high frame rate video is required. A good lighting system such as number of lighting point and orientation also plays a main role during the visual observation to capture a high quality image or video.

X-ray and gamma ray method

The X-radiography technique has been developed to overcome the refraction issue in visual observation. X-ray image can provide useful information on the nature of the flow whereas the image produced from the X-radiography depends only on the absorption. Thus, the flow characteristics can be easily acquired and understood from the x-ray images. Table-4 summarizes the experimental methods and applications that have been reported by the scholars.

Table-4: Experimental method and applications in determination of void fraction

Authors	Experiment	Application
Yu *et al*., [86]	Gamma ray attenuation	Focusing on Industrial application (boiler, core and steam generator in nuclear reactor)
Wang *et al*., [87]	Near Infrared Spectrum (NIR) technology	Natural gas production well oil-gas exploration and electricity generation.
Ying *et al*., [88]	Couple Contactless Conductivity Detection (C^4D)	Milimeter-scale devices/equipment
V.Sardeshpande *et al*., [89]	Electrical capacitance tomography and high speed photography	Industrial application
Srisomba *et al*., [90]	Quick-closing valve and optical observation	Air conditioning system, refrigerator
Winkler *et al*., [91]	Digital image processing	Air conditioning system, refrigerator
Paranjape *et al*., [92]	Electrical impedance-based	High-end electronic devices
Kim *et al*., [93]	Three ring conductance probe	Industrial application
Takenaka and Asano [94]	Umbra method using neutron absorber grid	Nuclear safety system
Lim *et al*., [95]	Neutron radiography	HANARO fuel channel
Yang *et al*., [96]	Impedance method	Industrial technologies application
Fukano [97]	Constant electric current method	Nuclear safety system

Jones and Zuber [98] utilized an X-ray beam that transmitted through the flow and its resultant intensity was determined in the detector. The output signal of the X-ray beam as a function of time was measured from the instantaneous void fraction and the probability density was used as a function for the determination of void fraction. Heindel *et al*., [99] applied an X-ray imaging method to differentiate and measure some flow characteristic in large vertical pipe with a maximum internal diameter of 32 cm and a height of 4 m. Their facilities included the x-ray radiography and a stereography imaging technique that enables the visualization of a 3D flow structure in an opaque channel with multiphase fluid flow with the rate of 60 frames per second. They used the digital detector to digitize the film radiography. Hu *et al*., [100] measured the void fraction distribution of phases and visualized the interfacial area structure by using the fast respond X-ray tomography. They found the amplitude wave that used to determine the liquid hold up in a stratified flow. Moreover, Nazemi *et al*., [80] measured the void fraction by neglecting the flow structure and used counted photon that sensed from the transmitted detector.

Electrical Method

Electrical method is the best measurement technique to measure the void fraction of flow inside the tube. This technique provides real time output from the experiment to measure the void fraction (Eq. 29) [92] as proposed by Uesawa et al. [79]. This electrical technique has been proposed by many researchers and resolved concurrent with the latest technology in the experimental field for measuring the void fraction [101, 102].

$$\alpha = \frac{v'-1}{v'} \tag{29}$$

Where

$v'(\equiv V'/V_0')$ is a voltage ratio.

This alternative way (electrical technique) used conductance probe was developed by Barnea *et al*., [29] to characterize the flow patterns. An insulated needle probe was inserted into the flow and the conductance between the needle probe tip and the tube wall was measured as a function of time. They obtained the characteristic of flow pattern by displaying the response detected from the flow through the oscilloscope. This method still has some disadvantages and which does not provide precise information as the contact between the needle probe and the flow can occur in all flow patterns.

Yoneda *et al*., [103] applied this technique for high temperature flow of steam-water in a vertical large diameter pipe with an internal diameter of 155-mm. The experiments were aimed to investigate the bubble characteristics and structure of the flow concerning the developing state of the flow. In the early stage of the experiment, most of the experiments were focused on the determination of flow pattern inside the tube. The data obtained from the experiment were useful and can be used to determine the void fraction [104].

Conductance probe is a real time measurement method to determine the void fraction and can also be used to calculate the heat transfer coefficient in two-phase flow. Typically, the conductance material functions as a sensor to capture the difference in the electrical conductivity of vapour and water phase in two-phase flow. Woroz *et al*., [105] used 13 two-phase flow condition and multi-sensor conductivity probe to measure velocity and interfacial area. They also introduced a new electrical circuit to improve the data capturing method in their experiments. This method was also employed by Serizawa *et al*., [106], Katoaka *et al*., [107], Cartellier, A. and Achard, J. L. [108], Wu, Q. and Ishii, M. [109] and Kim et. al. [110] to investigate the bubbly flow using the conductance probe. Serizawa *et al*., [106] found the flat radial profile was attributed to the ratio between the velocities of the phases over a huge portion of the fully developed bubbly flow.

Fossa [111] focused on the conductance technique to prove the performance of the ring-shaped and plate electrodes as a function of geometrical parameters, it would affect the void fraction gas-liquid in two-phase parameter. This research studied on the different probe geometries with making reference to annular, stratified and bubble phase distribution. It is a form of direct current method where the measured data does not require the reconstruction of cross sectional image with the distinctive reflection, which able to characterize gas and liquid phase. This technique had been employed by Tan *et al*., [112] for a flow pattern investigation of gas-liquid flow in a vertical arrangement. Nowadays, there are various advanced methods, which potential and useful for monitoring the flow pattern but it is still difficult to be applied in the real application of annular tube.

Future need and challenges in vapour-liquid condensation phenomena in annular tube

The heat transfer in different flow structures and the determination of void fraction via experimental method were reviewed in Sections 4 and 5, respectively. The review revealed that the influence of flow pattern and void fraction measurement method are significant in the knowledge enhancement of vapour-liquid condensation phenomena in the

annular tube. It also provides the fundamental knowledge and enhanced understanding of the importance of void fraction that gives the impact on the condensation behaviour of steam-water flow in the annular channel to the researcher and engineer. The review also revealed the empirical formula is useful in the prediction of bubble's radius and the effectiveness of the heat transfer that corresponded to the flow pattern. However, the empirical formula still has the limitation to predict the actual diameter and shape variation in various flow patterns and conditions, especially in a real time condition. This situation creates the challenges to the researcher to further explore the alternative method in this research field.

Aforementioned in Section 3, the real two-phase flow and condensation phenomena are difficult to visualize in the real application in the industry because of the non-transparent piping system. Moreover, the lack of proper equipment to visualize the flow and the phenomenon occur in the tube has restricted the researcher to carry out the experiment in the real industrial application. Besides, the void fraction of the flow is also difficult to measure in the non-transparent piping system. Therefore, a lab scale equipment or system was an alternative way to mimic the real piping system using a transparent pipe to investigate the two-phase flow and condensation phenomena. The review revealed several methods that have been employed to estimate the void fraction, which are (i) visual observation, (ii) x-ray and gamma ray and (iii) electrical method. With the aid of visualization tools (i.e., high speed camera), the flow pattern and the mechanism of two-phase flow can be easily recorded. The image of the flow can be analysed in the viewer software such as I-speed viewer. Even though flow mechanism can be captured in the experiment, this method only applicable to transparent pipe. Another alternative way that proposed by the researcher is the use of x-ray and gamma ray to visualize the 3D flow structure in the experiment. The x-ray technique is an effective way to estimate the flow inside the non-transparent tube and could provide the 3D flow structure. To further improve the x-ray technique in the visualization of flow structure and void fraction measurement, the portable feature must be added to the x-ray equipment to facilitate the researcher when dealing with the real industrial applications. The electrical method is a popular method that has been used by numerous researchers to estimate the void fraction through the conductance probe. The presence of bubble in the flow triggers the sensor, hence causes the difference of the electrical conductivity. Until today, the electrical method has only been applied in the lab scale analysis.

The review also revealed most of the experimental methods are limited to the lab scale that's not applicable to the industrial application, such as quick-closing valve and gamma ray. An alternative method using the ultrasonic [113-118] was reported by a few researchers. Ultrasonic is the practical technique that needs to develop in analysing the void fraction and heat transfer or phase change phenomena. Acoustic properties [105] were used to detect the bubble volumetric void fraction. Besides, ultrasonic vibration can intensify the occurrence of bubbles. Ultrasonic equipment (e.g., multiwave ultrasonic pulsed Doppler [107] and multiwave transducer [110] was employed to measure the bubble velocity profile. However, this equipment is limited in the measurement of cross-sectional area of the bubble. Thus, cross-correlation method [110] was introduced with the aid of high-speed camera to capture the bubble size. The advantages of using ultrasonic method are (i) does not require additional fabrication to measure two-phase flow variable (void fraction and flow pattern) and (ii) able to provide both result instantaneously (picture and measurement). Even though the ultrasonic method with cross-correlation method provides effective velocity and cross-sectional measurement of the bubble, this method still has a limitation to be applied in the industry. Therefore, this remains a huge gap and challenges to the researcher. The researcher needs to focus on the improvement of the ultrasonic method towards the application in the industry. This review also revealed that the current measurement techniques mostly need a custom fabrication and development to fit in the transparent tube, this situation restraint the implementation in the real industrial application. The enhancement of the void fraction measurement and new visualization technologies for the condensation phenomena pose challenges to engineers and researchers.

CONCLUSIONS

Reviews on the vapour-liquid condensation phenomena in annular tube were presented in this article based on the substantial previous works. Vapour-liquid condensation phenomena in an annular tube are crucial in the heat transfer of two-phase flow. The determination of the heat transfer in an annular tube was classified in two categories, namely analytical and experimental techniques. Heat transfer in different flow structures and determination of void fraction methods have also been reviewed and presented. Various heat transfer empirical equations were proposed based on the different flow structures (i.e., bubbly and slug flow) to describe the two-phase flow. Reynolds and Prandtl number of the flow inside the annular tube was considered in the empirical equation to represent the flow condition. The challenges in the measurement and visualization of the vapour-liquid condensation phenomena are (i) complexity of the two-phase flow, (ii) limited real-time equipment, (iii) lab-scaled equipment and (iv) portable 3D imaging or scanning device for bubble characterization. The complexity of the two-phase flow and vapour-liquid condensation phenomenon led to the difficulties in the experimental work because of the irregular changes of void fraction in the flow. A few research gaps exist in the determination of the void fraction and heat transfer in the two-phase flow via experiment, including (i) the real time measurement of entire bubble void fractions, (ii) the variation of bubble characteristics during the phase change and (iii) the use of portable 3D imaging in the real industrial applications. The realization of the suggested experimental

techniques could guarantee significant enhancement in the determination of void fraction and visualization of vapour-liquid condensation phenomenon. Thus, the collaboration of engineers and researchers from both industrial and academic institutions is essential in achieving the successful knowledge advancement.

REFERENCES

1. Nusselt, W. (1916). Die oberflachenkondensation des wasserdampfes. *VDI Z*, *60*, 541-546.
2. Zhang, C., Shen, C., & Chen, Y. (2017). Experimental study on flow condensation of mixture in a hydrophobic microchannel. *International Journal of Heat and Mass Transfer*, *104*, 1135-1144.
3. Xu, Q., Guo, L., & Chang, L. (2017). Interfacial characteristics of steam jet condensation in crossflow of water in a vertical pipe. *Applied Thermal Engineering*, *113*, 1266-1276.
4. Gou, J., Wang, B., & Shan, J. (2017). Development of an analytical model for pure vapor downflow condensation in a vertical tube. *Nuclear Engineering and Design*, *320*, 346-360.
5. Azizi, S., & Ahmadloo, E. (2016). Prediction of heat transfer coefficient during condensation of R134a in inclined tubes using artificial neural network. *Applied Thermal Engineering*, *106*, 203-210.
6. Chantana, C., & Kumar, S. (2013). Experimental and theoretical investigation of air-steam condensation in a vertical tube at low inlet steam fractions. *Applied Thermal Engineering*, *54*(2), 399-412.
7. Yao, W., & Morel, C. (2004). Volumetric interfacial area prediction in upward bubbly two-phase flow. *International Journal of Heat and Mass Transfer*, *47*(2), 307-328.
8. Quan, X., Cheng, P., & Wu, H. (2008). Transition from annular flow to plug/slug flow in condensation of steam in microchannels. *International Journal of Heat and Mass Transfer*, *51*(3-4), 707-716.
9. Tangren, R. F., Dodge, C. H., & Seifert, H. S. (1949). Compressibility effects in two-phase flow. *Journal of Applied Physics*, *20*(7), 637-645.
10. Albagli, D., & Gany, A. (2003). High speed bubbly nozzle flow with heat, mass, and momentum interactions. *International Journal of Heat and Mass Transfer*, *46*(11), 1993-2003.
11. Zehtabiyan-Rezaie, N., Saffar-Avval, M., & Mirzaei, M. (2015). Analytical and numerical investigation of heat transfer and entropy generation of stratified two-phase flow in mini-channel. *International Journal of Thermal Sciences*, *90*, 24-37.
12. Jeong, K., Kessen, M. J., Bilirgen, H., & Levy, E. K. (2010). Analytical modeling of water condensation in condensing heat exchanger. *International Journal of Heat and Mass Transfer*, *53*(11-12), 2361-2368.
13. Kubín, M., Hirš, J., & Plášek, J. (2016). Experimental analysis of steam condensation in vertical tube with small diameter. *International Journal of Heat and Mass Transfer*, *94*, 403-410.
14. Kim, H., Kwon, T. S., & Kim, D. E. (2016). Experimental study of air-cooled water condensation in slightly inclined circular tube using infrared temperature measurement technique. *Nuclear Engineering and Design*, *308*, 38-50.
15. Qu, X. H., Sui, H., & Tian, M. C. (2016). CFD simulation of steam–air jet condensation. *Nuclear Engineering and Design*, *297*, 44-53.
16. El Mghari, H., & Louahlia-Gualous, H. (2016). Experimental and numerical investigations of local condensation heat transfer in a single square microchannel under variable heat flux. *International Communications in Heat and Mass Transfer*, *71*, 197-207.
17. Zeng, Q., Cai, J., Yin, H., Yang, X., & Watanabe, T. (2015). Numerical simulation of single bubble condensation in subcooled flow using OpenFOAM. *Progress in Nuclear Energy*, *83*, 336-346.
18. El Nakla, M., Al-Sarkhi, A., & Alsurakji, I. (2013). A look-up table for two-phase frictional pressure drop multiplier. *Nuclear Engineering and Design*, *265*, 450-468.
19. Lee, K. Y., & Kim, M. H. (2008). Effect of an interfacial shear stress on steam condensation in the presence of a noncondensable gas in a vertical tube. *International Journal of Heat and Mass Transfer*, *51*(21-22), 5333-5343.
20. Gjennestad, M. A., & Munkejord, S. T. (2015). Modelling of heat transport in two-phase flow and of mass transfer between phases using the level-set method. *Energy Procedia*, *64*, 53-62.
21. Whitley, R. H., Chan, C. K., & Okrent, D. (1976). On the analysis of containment heat transfer following a LOCA. *Annals of Nuclear Energy*, *3*(11-12), 515-525.
22. Chan, S. H., Cho, D. H., & Condiff, D. W. (1980). Heat transfer from a high temperature condensable mixture. *International Journal of Heat and Mass Transfer*, *23*(1), 63-71.
23. Chitti, M. S., & Anand, N. K. (1995). An analytical model for local heat transfer coefficients for forced convective condensation inside smooth horizontal tubes. *International journal of heat and mass transfer*, *38*(4), 615-627.
24. Hewitt, G. F., & Roberts, D. N. (1969). *Studies of two-phase flow patterns by simultaneous x-ray and flast photography*(No. AERE-M--2159). Atomic Energy Research Establishment, Harwell, England (United Kingdom).
25. Collier, J. G. Convective Boiling and Condensation, McGraw-Hill, New York, 1981.
26. Fair, J. R. (1960). *What you need to design thermosiphon reboilers*.
27. Dalkilic, A. S., & Wongwises, S. (2010). An investigation of a model of the flow pattern transition mechanism in relation to the identification of annular flow of R134a in a vertical tube using various void fraction models and flow regime maps. *Experimental Thermal and Fluid Science*, *34*(6), 692-705.

28. Taitel, Y., & Dukler, A. E. (1976). A model for predicting flow regime transitions in horizontal and near horizontal gas-liquid flow. *AIChE Journal*, *22*(1), 47-55.
29. Barnea, D., Shoham, O., & Taitel, Y. (1980). Flow pattern characterization in two phase flow by electrical conductance probe. *International Journal of Multiphase Flow*, *6*(5), 387-397.
30. Furukawa, T., & Fukano, T. (2001). Effects of liquid viscosity on flow patterns in vertical upward gas–liquid two-phase flow. *International journal of multiphase flow*, *27*(6), 1109-1126.
31. Kattan, N., Thome, J. R., & Favrat, D. (1998). Flow boiling in horizontal tubes: Part 1—Development of a diabatic two-phase flow pattern map. *Journal of heat transfer*, *120*(1), 140-147.
32. Zürcher, O., Favrat, D., & Thome, J. R. (2002). Development of a diabatic two-phase flow pattern map for horizontal flow boiling. *International Journal of Heat and Mass Transfer*, *45*(2), 291-301.
33. Dalkilic, A. S., & Wongwises, S. (2009). Intensive literature review of condensation inside smooth and enhanced tubes. *International Journal of Heat and Mass Transfer*, *52*(15-16), 3409-3426.
34. Rouhani, S. Z., & Axelsson, E. (1970). Calculation of void volume fraction in the subcooled and quality boiling regions. *International Journal of Heat and Mass Transfer*, *13*(2), 383-393.
35. Liang, K. S. (1994). Experimental and analytical study of direct contact condensation of steam in water. *Nuclear Engineering and Design*, *147*(3), 425-435.
36. Kalman, H., & Mori, Y. H. (2002). Experimental analysis of a single vapor bubble condensing in subcooled liquid. *Chemical Engineering Journal*, *85*(2-3), 197-206.
37. Tang, J., Yan, C., Sun, L., Li, Y., & Wang, K. (2015). Effect of liquid subcooling on acoustic characteristics during the condensation process of vapor bubbles in a subcooled pool. *Nuclear Engineering and Design*, *293*, 492-502.
38. Qu, X. H., Tian, M. C., Zhang, G. M., & Leng, X. L. (2015). Experimental and numerical investigations on the air–steam mixture bubble condensation characteristics in stagnant cool water. *Nuclear Engineering and Design*, *285*, 188-196.
39. Owoeye, E. J., & Schubring, D. (2015). Numerical simulation of vapor bubble condensation in turbulent subcooled flow boiling. *Nuclear Engineering and Design*, *289*, 126-143.
40. Al Issa, S., Weisensee, P., & Macián-Juan, R. (2014). Experimental investigation of steam bubble condensation in vertical large diameter geometry under atmospheric pressure and different flow conditions. *International Journal of Heat and Mass Transfer*, *70*, 918-929.
41. Al Issa, S., Weisensee, P., & Macián-Juan, R. (2014). Experimental investigation of steam bubble condensation in vertical large diameter geometry under atmospheric pressure and different flow conditions. *International Journal of Heat and Mass Transfer*, *70*, 918-929.
42. Inaba, N., Watanabe, N., & Aritomi, M. (2013). Interfacial heat transfer of condensation bubble with consideration of bubble number distribution in subcooled flow boiling. *Journal of Thermal Science and Technology*, *8*(1), 74-90.
43. Lucas, D., & Prasser, H. M. (2007). Steam bubble condensation in sub-cooled water in case of co-current vertical pipe flow. *Nuclear Engineering and Design*, *237*(5), 497-508.
44. Kim, S. J., & Park, G. C. (2011). Interfacial heat transfer of condensing bubble in subcooled boiling flow at low pressure. *International Journal of Heat and Mass Transfer*, *54*(13-14), 2962-2974.
45. Sakamatapan, K., Kaew-On, J., Dalkilic, A. S., Mahian, O., & Wongwises, S. (2013). Condensation heat transfer characteristics of R-134a flowing inside the multiport minichannels. *International journal of heat and mass transfer*, *64*, 976-985.
46. Isenberg, J., & Sideman, S. (1970). Direct contact heat transfer with change of phase: bubble condensation in immiscible liquids. *International Journal of Heat and Mass Transfer*, *13*(6), 997-1011.
47. AKIYAMA, M. (1973). Bubble collapse in subcooled boiling. *Bulletin of JSME*, *16*(93), 570-575.
48. Chen, Y. M., & Mayinger, F. (1992). Measurement of heat transfer at the phase interface of condensing bubbles. *International journal of multiphase flow*, *18*(6), 877-890.
49. Zeitoun, O., Shoukri, M., & Chatoorgoon, V. (1994). Measurement of interfacial area concentration in subcooled liquid-vapour flow. *Nuclear Engineering and Design*, *152*(1-3), 243-255.
50. Ranz, W. E., & Marshall, W. R. (1952). Evaporation from drops. *Chem. Eng. Prog*, *48*(3), 141-146.
51. Hughmark, G. A. (1967). Mass and heat transfer from rigid spheres. *AIChE Journal*, *13*(6), 1219-1221.
52. Kim, S. M., & Mudawar, I. (2013). Universal approach to predicting heat transfer coefficient for condensing mini/micro-channel flow. *International Journal of Heat and Mass Transfer*, *56*(1-2), 238-250.
53. Warrier, G. R., Basu, N., & Dhir, V. K. (2002). Interfacial heat transfer during subcooled flow boiling. *International Journal of Heat and Mass Transfer*, *45*(19), 3947-3959.
54. Akers, W. W., Deans, H. A., & Crosser, O. K. (1958). Condensing heat transfer within horizontal tubes. *Chem. Eng. Progr.*, *54*.
55. Cavallini, A., & Zecchin, R. (1974, September). A dimensionless correlation for heat transfer in forced convection condensation. In *Proceedings of the Sixth International Heat Transfer Conference* (Vol. 3, pp. 309-313).
56. Shah, M. M. (1979). A general correlation for heat transfer during film condensation inside pipes. *International Journal of heat and mass transfer*, *22*(4), 547-556.

57. Haraguchi, H. (1994). Condensation of refrigerants HCFC22, HFC134a and HCFC123 in a horizontal smooth tube. *Transactions of the Japan Society of Mechanical Engineers*, *60*(574), 245-252.
58. Dobson, M. K., & Chato, J. C. (1998). Condensation in smooth horizontal tubes. *Journal of Heat Transfer*, *120*(1), 193-213.
59. Wang, W. W. W., Radcliff, T. D., & Christensen, R. N. (2002). A condensation heat transfer correlation for millimeter-scale tubing with flow regime transition. *Experimental Thermal and Fluid Science*, *26*(5), 473-485.
60. Koyama, S., Kuwahara, K., & Nakashita, K. (2003, January). Condensation of refrigerant in a multi-port channel. In *ASME 2003 1st International Conference on Microchannels and Minichannels* (pp. 193-205). American Society of Mechanical Engineers.
61. Lin, C. H., & Hibiki, T. (2014). Databases of interfacial area concentration in gas–liquid two-phase flow. *Progress in Nuclear Energy*, *74*, 91-102.
62. Ma, K., Guo, L., & Wang, Y. (2015). Interfacial area transport of subcooled water–steam condensing bubbly flow in vertical pipe. *International Journal of Heat and Mass Transfer*, *86*, 78-89.
63. Yang, X., Schlegel, J. P., Liu, Y., Paranjape, S., Hibiki, T., Ishii, M., ... & Ireland, A. (2016). Prediction of interfacial area transport in a scaled 8× 8 BWR rod bundle. *Nuclear Engineering and Design*, *310*, 638-647.
64. Rohatgi, U. S., & Saha, P. (1980). *Constitutive relations in TRAC-P1A* (No. NUREG/CR-1651; BNL-NUREG-51258). Brookhaven National Lab., Upton, NY (USA).
65. Zuber, N., & Findlay, J. (1965). Average volumetric concentration in two-phase flow systems. *Journal of heat transfer*, *87*(4), 453-468.
66. Toda, S., & Hori, Y. (1993). Characteristics of two-phase condensing flow by visualization using computed image processing. *Nuclear engineering and design*, *141*(1-2), 35-46.
67. Kasturi, G., & Stepanek, J. B. (1974). Two-phase flow—IV. Gas and liquid side mass transfer coefficients. *Chemical Engineering Science*, *29*(9), 1849-1856.
68. Akita, K., & Yoshida, F. (1974). Bubble size, interfacial area, and liquid-phase mass transfer coefficient in bubble columns. *Industrial & Engineering Chemistry Process Design and Development*, *13*(1), 84-91.
69. Tomida, T., Yusa, F., & Okazaki, T. (1978). Effective interfacial area and liquid—side mass transfer coefficient in the upward two-phase flow of gas—liquid mixtures. *The Chemical Engineering Journal*, *16*(2), 81-88.
70. Yun, B. J., Bae, B. U., Euh, D. J., Park, G. C., & Song, C. H. (2010). Characteristics of the local bubble parameters of a subcooled boiling flow in an annulus. *Nuclear Engineering and Design*, *240*(9), 2295-2303.
71. Ho, M. K. M., Yeoh, G. H., & Tu, J. Y. (2008). Population balance models for subcooled boiling flows. *International Journal of Numerical Methods for Heat & Fluid Flow*, *18*(2), 160-172.
72. Yeoh, G. H., & Tu, J. Y. (2006). Two-fluid and population balance models for subcooled boiling flow. *Applied mathematical modelling*, *30*(11), 1370-1391.
73. Park, H. S., No, H. C., & Bang, Y. S. (2003). Analysis of experiments for in-tube steam condensation in the presence of noncondensable gases at a low pressure using the RELAP5/MOD3. 2 code modified with a non-iterative condensation model. *Nuclear Engineering and Design*, *225*(2-3), 173-190.
74. Keska, J. K., & Williams, B. E. (1999). Experimental comparison of flow pattern detection techniques for air–water mixture flow. *Experimental Thermal and Fluid Science*, *19*(1), 1-12.
75. Brooks, C. S., Ozar, B., Hibiki, T., & Ishii, M. (2014). Interfacial area transport of subcooled boiling flow in a vertical annulus. *Nuclear Engineering and Design*, *268*, 152-163.
76. Ozar, B., Brooks, C. S., Hibiki, T., & Ishii, M. (2013). Interfacial area transport of vertical upward steam–water two-phase flow in an annular channel at elevated pressures. *International Journal of Heat and Mass Transfer*, *57*(2), 504-518.
77. Ko, M. S., Lee, B. A., Won, W. Y., Lee, Y. G., Jerng, D. W., & Kim, S. (2015). An improved electrical-conductance sensor for void-fraction measurement in a horizontal pipe. *Nuclear Engineering and Technology*, *47*(7), 804-813.
78. Tsutsumi, T., Takeuchi, S., & Kajishima, T. (2014). Heat transfer and particle behaviours in dispersed two-phase flow with different heat conductivities for liquid and solid. *Flow, turbulence and combustion*, *92*(1-2), 103-119.
79. Uesawa, S. I., Kaneko, A., & Abe, Y. (2012). Measurement of void fraction in dispersed bubbly flow containing micro-bubbles with the constant electric current method. *Flow measurement and instrumentation*, *24*, 50-62.
80. Nazemi, E., Feghhi, S. A. H., Roshani, G. H., Peyvandi, R. G., & Setayeshi, S. (2016). Precise void fraction measurement in two-phase flows independent of the flow regime using gamma-ray attenuation. *Nuclear Engineering and Technology*, *48*(1), 64-71.
81. Bruvik, E. M., Hjertaker, B. T., & Hallanger, A. (2010). Gamma-ray tomography applied to hydro-carbon multi-phase sampling and slip measurements. *flow measurement and instrumentation*, *21*(3), 240-248.
82. Richter, T., Eckert, K., Yang, X., & Odenbach, S. (2015). Measuring the diameter of rising gas bubbles by means of the ultrasound transit time technique. *Nuclear Engineering and Design*, *291*, 64-70.
83. Tamura, Y., Tsurumi, N., & Matsumoto, Y. (2014). Visualizations of bubble motions and temperature rises by focused ultrasound. *Procedia Engineering*, *90*, 5-10.
84. Taylor, N. H., & Hewitt, G. F. (1963). The motion and frequency of large disturbance waves in annular two-phase flow of air-water mixtures. *Chemical Engineering Science*, *18*(8), 537-552.

85. Kim, S., Sun, X., Ishii, M., Beus, S. G., & Lincoln, F. (2003). Interfacial area transport and evaluation of source and sink terms for confined air–water bubbly flow. *Nuclear engineering and design*, *219*(1), 61-75.
86. Zhao, Y., Bi, Q., Yuan, Y., & Lv, H. (2016). Void fraction measurement in steam–water two-phase flow using the gamma ray attenuation under high pressure and high temperature evaporating conditions. *Flow Measurement and Instrumentation*, *49*, 18-30.
87. Wang, C., Zhao, N., Fang, L., Zhang, T., & Feng, Y. (2016). Void fraction measurement using NIR technology for horizontal wet-gas annular flow. *Experimental Thermal and Fluid Science*, *76*, 98-108.
88. Zhou, Y., Huang, Z., Wang, B., Ji, H., & Li, H. (2015). A new method for void fraction measurement of gas–liquid two-phase flow in millimeter-scale pipe. *International Journal of Multiphase Flow*, *72*, 298-305.
89. Sardeshpande, M. V., Harinarayan, S., & Ranade, V. V. (2015). Void fraction measurement using electrical capacitance tomography and high speed photography. *Chemical Engineering Research and Design*, *94*, 1-11.
90. Srisomba, R., Mahian, O., Dalkilic, A. S., & Wongwises, S. (2014). Measurement of the void fraction of R-134a flowing through a horizontal tube. *International Communications in Heat and Mass Transfer*, *56*, 8-14.
91. Winkler, J., Killion, J., & Garimella, S. (2012). Void fractions for condensing refrigerant flow in small channels. Part II: Void fraction measurement and modeling. *International journal of refrigeration*, *35*(2), 246-262.
92. Paranjape, S., Ritchey, S. N., & Garimella, S. V. (2012). Electrical impedance-based void fraction measurement and flow regime identification in microchannel flows under adiabatic conditions. *International Journal of Multiphase Flow*, *42*, 175-183.
93. Kim, J., Ahn, Y. C., & Kim, M. H. (2009). Measurement of void fraction and bubble speed of slug flow with three-ring conductance probes. *Flow Measurement and Instrumentation*, *20*(3), 103-109.
94. Takenaka, N., & Asano, H. (2005). Quantitative CT-reconstruction of void fraction distributions in two-phase flow by neutron radiography. *Nuclear Instruments and Methods in Physics Research Section A: Accelerators, Spectrometers, Detectors and Associated Equipment*, *542*(1-3), 387-391.
95. Lim, I. C., Sim, C. M., Cha, J. E., Choi, Y. S., Takenaka, N., Saito, Y., & Jun, B. J. (2005). Measurement of the void fraction in a channel simulating the HANARO fuel assembly using neutron radiography. *Nuclear Instruments and Methods in Physics Research Section A: Accelerators, Spectrometers, Detectors and Associated Equipment*, *542*(1-3), 181-186.
96. Yang, H. C., Kim, D. K., & Kim, M. H. (2003). Void fraction measurement using impedance method. *Flow Measurement and Instrumentation*, *14*(4-5), 151-160.
97. Fukano, T. (1998). Measurement of time varying thickness of liquid film flowing with high speed gas flow by a constant electric current method (CECM). *Nuclear Engineering and Design*, *184*(2-3), 363-377.
98. Jones Jr, O. C., & Zuber, N. (1975). The interrelation between void fraction fluctuations and flow patterns in two-phase flow. *International Journal of Multiphase Flow*, *2*(3), 273-306.
99. Heindel, T. J., Gray, J. N., & Jensen, T. C. (2008). An X-ray system for visualizing fluid flows. *Flow Measurement and Instrumentation*, *19*(2), 67-78.
100. Hu, B., Langsholt, M., Liu, L., Andersson, P., & Lawrence, C. (2014). Flow structure and phase distribution in stratified and slug flows measured by X-ray tomography. *International Journal of Multiphase Flow*, *67*, 162-179.
101. Perera, K., Pradeep, C., Mylvaganam, S., & Time, R. W. (2017). Imaging of oil-water flow patterns by Electrical Capacitance Tomography. *Flow Measurement and Instrumentation*, *56*, 23-34.
102. Kim, B. S., & Kim, K. Y. (2017). Resistivity imaging of binary mixture using weighted Landweber method in electrical impedance tomography. *Flow Measurement and Instrumentation*, *53*, 39-48.
103. Yoneda, K., Yasuo, A., & Okawa, T. (2002). Bubble characteristics of steam–water two-phase flow in a large-diameter pipe. *Experimental thermal and fluid science*, *26*(6-7), 669-676.
104. Thome, J. R., Bar-Cohen, A., Revellin, R., & Zun, I. (2013). Unified mechanistic multiscale mapping of two-phase flow patterns in microchannels. *Experimental Thermal and Fluid Science*, *44*, 1-22.
105. Worosz, T., Bernard, M., Kong, R., Toptan, A., Kim, S., & Hoxie, C. (2016). Sensitivity studies on the multi-sensor conductivity probe measurement technique for two-phase flows. *Nuclear Engineering and Design*, *310*, 552-563.
106. Serizawa, A. (1975). *Turbulence Structure of Air-Water Bubbly Flow -II. Local Properties.* International Journal of Multiphase Flow. **2**: p. 254-246.
107. Kataoka, I., Ishii, M., & Serizawa, A. (1986). Local formulation and measurements of interfacial area concentration in two-phase flow. *International Journal of Multiphase Flow*, *12*(4), 505-529.
108. Cartellier, A., & Achard, J. L. (1991). Local phase detection probes in fluid/fluid two-phase flows. *Review of Scientific Instruments*, *62*(2), 279-303.
109. Wu, Q., & Ishii, M. (1999). Sensitivity study on double-sensor conductivity probe for the measurement of interfacial area concentration in bubbly flow. *International Journal of Multiphase Flow*, *25*(1), 155-173.
110. Kim, S., Fu, X. Y., Wang, X., & Ishii, M. (2000). Development of the miniaturized four-sensor conductivity probe and the signal processing scheme. *International journal of heat and mass transfer*, *43*(22), 4101-4118.
111. Fossa, M. (1998). Design and performance of a conductance probe for measuring the liquid fraction in two-phase gas-liquid flows. *Flow Measurement and Instrumentation*, *9*(2), 103-109.

112. Tan, C., Dong, F., & Wu, M. (2007). Identification of gas/liquid two-phase flow regime through ERT-based measurement and feature extraction. *Flow Measurement and Instrumentation*, *18*(5-6), 255-261.
113. Sastre, M. T. T., & Vanhille, C. (2017). A numerical model for the study of the difference frequency generated from nonlinear mixing of standing ultrasonic waves in bubbly liquids. *Ultrasonics sonochemistry*, *34*, 881-888.
114. Tang, J., Yan, C., & Sun, L. (2015). Effects of noncondensable gas and ultrasonic vibration on vapor bubble condensing and collapsing. *Experimental Thermal and Fluid Science*, *61*, 210-220.
115. Nguyen, T. T., Kikura, H., Murakawa, H., & Tsuzuki, N. (2015). Measurement of bubbly two-phase flow in vertical pipe using multiwave ultrasonic pulsed Dopller method and wire mesh tomography. *Energy Procedia*, *71*, 337-351.
116. Merouani, S., Hamdaoui, O., Rezgui, Y., & Guemini, M. (2015). Sensitivity of free radicals production in acoustically driven bubble to the ultrasonic frequency and nature of dissolved gases. *Ultrasonics sonochemistry*, *22*, 41-50.
117. Hetsroni, G., Moldavsky, L., Fichman, M., Pogrebnyak, E., & Mosyak, A. (2014). Ultrasonic enhancement of subcooled pool boiling of freely oscillated wires. *International Journal of Multiphase Flow*, *67*, 13-21.
118. Murakawa, H., Kikura, H., & Aritomi, M. (2008). Application of ultrasonic multi-wave method for two-phase bubbly and slug flows. *Flow measurement and instrumentation*, *19*(3-4), 205-213.